PHYSICAL REVIEW B VOLUME 24, NUMBER 4 15 AUGUST 1981

Transport and optical properties of $Ti_{1+x}S_2$

Carl A. Kukkonen, W. J. Kaiser, and E. M. Logothetis
Engineering and Research Staff, Ford Motor Company, Dearborn, Michigan 48121

B. J. Blumenstock and P. A. Schroeder
Physics Department, Michigan State University, East Lansing, Michigan 48824

S. P. Faile, R. Colella, and J. Gambold
Department of Physics, Purdue University, West Lafayette, Indiana 47907
(Received 2 September 1980)

We report measurements of the electrical resistivity, Hall coefficient, magnetoresistance, thermoelectric power, infrared reflectivity, and c-axis lattice parameter of single crystals of titanium disulfide $Ti_{1+x}S_2$ with varying degrees of nonstoichiometry. The strong correlations we find between different measurements made on the same sample allow us to conclude that titanium disulfide is a semiconductor rather than a semimetal. Even though this fact is established, our most stoichiometric samples continue to exhibit metallic behavior, and the source of these conduction electrons is unknown. In addition, none of the scattering mechanisms examined here is capable of explaining the unusual temperature dependence of the electrical resistivity which varies as T^3 at low T and as T^y above 100 K where y ranges from 1.85 for the least stoichiometric samples to 2.2 for the most stoichiometric.

I. INTRODUCTION

We report the results of extensive measurements of the physical properties of single crystals of titanium disulfide $Ti_{1+x}S_2$ with varying degrees of nonstoichiometry. The quantities investigated are the electrical resistivity, Hall coefficient, magnetoresistance, thermoelectric power, infrared reflectivity, and c-axis lattice parameter. Each of these measurements was made on the same single crystal (or on crystals from the same batch). With this procedure, it is possible to establish strong correlations among the results for samples with different nonstoichiometry. These correlations are consistent with the extrinsic semiconductor model of TiS_2 but are inconsistent with a semimetal.

Takeuchi and Katsuta[1] were the first to propose that TiS_2 was a semimetal with the charge carriers (electrons and holes) arising from the intrinsic overlap of the sulfur $3p$ valence band with the titanium $3d$ conduction band. This view was endorsed by Thompson *et al.* who found that highly stoichiometric $Ti_{1+x}S_2$ ($x \leq 0.001$) continued to exhibit metallic conductivity. Thompson *et al.*[2] also claimed that the magnetic transport and optical properties consistently suggested that TiS_2 was a semimetal rather than an extrinsic semiconductor. The semimetallic model, however, was vigorously challenged by Wilson,[3,4] who argued that the data of Thompson *et al.*[2] could be accommodated within the original view that TiS_2 was a dirty extrinsic semiconductor.

This semimetal-versus-semiconductor controversy was one of the major issues that stimulated the present lengthy investigation. In addition to our own work, which shows that TiS_2 is a semiconductor, two other groups have independently reached the same conclusion. Friend *et al.*[5] measured the pressure dependence of the Hall coefficient and Chen *et al.*[6] used angular-resolved photoemission. Taken together, all these results provide overwhelming evidence that TiS_2 is indeed a semiconductor.

Even though the semiconducting nature of TiS_2 is established, many mysteries remain. Our most stoichiometric samples continue to exhibit metallic behavior with an electron concentration of $2.2 \times 10^{20}/cm^3$. The source of these (extrinsic) carriers is unknown. The temperature dependence of the electrical resistivity, ρ, is also anomalous. Although previous data reported that the resistivity of TiS_2 varied with temperature as T^2 from 10 to 400 K due to electron-electron scattering,[7] our results show that below about 40 K ρ varies as T^3 regardless of sample stoichiometry; the temperature dependence at high temperatures depends on stoichiometry and has the approximate from $\rho \propto T^y$

from about 100 to 700 K, where y ranges from 1.85 for the least stoichiometric sample to 2.2 for the most stoichiometric. This temperature dependence and the electron-density dependence of the resistivity we observe are not consistent with simple electron-electron scattering. However, none of the scattering mechanisms examined here is capable of explaining the data.

The magnetoresistance of $Ti_{1+x}S_2$ is also unusual. Its magnitude and sign appear to depend on subtle differences between samples which do not affect other physical properties. We also find that the lattice parameter of our most-stoichiometric single crystals is larger than that reported for stoichiometric TiS_2 powder,[2] and the thermoelectric power for the same crystal is smaller than that for the powder.[2]

This paper describes the material preparation and characterization procedures (Sec. II), the physical measurements (Sec. III), and the data analysis and conclusions (Sec. IV). A brief summary of our results was presented previously in a Letter[8] and at the International Conference on Layered Compounds and Intercalates[9] In this publication, our measurements, results, and analysis are presented in sufficient detail to provide the reader with convincing evidence for the validity of the semiconducting model for TiS_2. This amount of detail is also necessary because our results differ significantly with some previous work and because we wish to demonstrate clearly that none of the conventional scattering mechanisms is capable of explaining our resistivity data.

II. MATERIAL PREPARATION AND CHARACTERIZATION

Single crystals of titanium disulfide were grown by the vapor-transport technique with sulfur or iodine as the transport agent. The starting TiS_2 powders were either commercially obtained (99.5% pure from Cerac/Pure, Inc. with the following major metallic impurities in ppm by weight: 0.03 Si, 0.1 Fe, and 0.1 Cu) or prepared in-house by reaction of 99.9999% pure sulfur with 99.97% pure titanium wire. In a typical crystal-growth run, a charge of TiS_2 powder (~ 5 g) was placed at one end of an evacuated quartz tube (~ 10 in. long, 1 in diameter) together with iodine or sulfur (a few mg/cm^3). The transport was achieved by establishing a $75-100\,^{\circ}$C temperature gradient along the tube with the powder at the hot end and growth occurring at the cool end. Highly stoichiometric crystals were obtained when the growth temperature was near $650\,^{\circ}$C.[2] Lower temperatures tended to produce unwanted whiskers of TiS_3. Higher temperature resulted in increasingly nonstoichiometric $Ti_{1+x}S_2$. Growth times varied from a few days to a month. Table I shows the growth conditions, the c-axis lattice parameter, and the carrier concentration (determined from the Hall coefficient assuming a single carrier with effective mass equal to the free-electron mass) for a number of titanium disulfide single crystals. The single-crystal batch numbers correspond to those given in Refs. 8 and 9. The crystals designated as Exxon were provided by A. H. Thompson of Exxon Research and Engineering Company as an example of their highly stoichiometric material. Because of an insufficient quantity of single crystals, no attempt was made to determine directly the stoichiometry of our materials by such means as chemical analysis. However, as discussed in later sections, certain inferences concerning stoichiometry can be made from measurements of the thermoelectric power, carrier concentration, and lattice constant. A mass spectrographic analysis of a crystal grown from the commercial powder with iodine as the transport agent identified the following major impurities (in ppm) by weight: Cl (500), Cu (100), Si (50), Sn (50), Fe (30), Mn (20), and I (100). The chlorine contamination presumably originates from commercial powder but this low level could not significantly affect our following conclusions. Note the low level of iodine incorporation.

The c-axis lattice parameter d of the single crystals shown in Table I was determined by x-ray diffraction using the Bond method.[10] In this method, one measures Bragg reflections with θ close to 90° on both sides of the incident beam. The advantages of this method are the high accuracy in measuring the lattice spacing and the fact that knowledge of the zero in the scale on which θ is measured is not required. All measurements were made on crystals with mosaic spread not exceeding $10-12$ minutes of arc. All determinations were based on the 008 reflection using the Cu $K\beta$ radiation. A fine slit was placed between the crystal and the x-ray source, whereas the counter aperture was left wide open. The c-axis lattice parameters of several different crystals from the same batch were measured and the variations within the batch did not exceed the error bars associated with one single measurement. The uncertainty reported in Table I is a conservative estimate and represents $\Delta d/d$ of about 10^{-4}.

The lattice parameter of the highly stoichiometric Exxon crystal was found to be 5.6978 ± 0.0006. This value is considerably higher than the reported

TABLE I. Growth conditions c-axis lattice parameter, and carrier concentration of $Ti_{1+x}S_2$ single crystals having varying degrees of nonstoichiometry.

Single-crystal batch no.	Growth conditions	c-axis lattice parameter	Electron concentration[b] (10^{20} cm^{-3})
164	Powder from elements sulfur transport growth temp. = 650 °C	5.6982 ± 6 5.6993 ± 13[a]	2.2
9	Powder from elements sulfur transport growth temp. = 600 °C	5.6984 ± 6	2.2
6	Powder from elements sulfur transport growth temp. = 700 °C	5.6986 ± 8	3.0
3	Commerical powder iodine transfer growth temp. = 700 °C	5.7001 ± 9	7.5
7	Powder from elements iodine transfer growth temp. = 700 °C	5.6991 ± 7	7.5
8	Commerical powder iodine transfer growth temp. = 800 °C	5.7008 ± 6	1.3
1	Commerical powder iodine transport growth temp. = 900 °C	5.7043 ± 8	3.4
Exxon		5.6978 ± 6	2.4

[a]Measured on powder from crushed single crystal.
[b]Calculated from the room-temperature Hall coefficient.

value of 5.6953 ± 0.0002 for stoichiometric TiS_2.[2] However, the latter was measured on powders rather than single crystals. This apparent inconsistency led us to check the accuracy of the single-crystal measurement by deliberately crushing one crystal from batch no. 164 to a very fine powder and measuring its lattice parameter using a powder diffractometer. In this measurement, the inherent accuracy was of the order of $\Delta d/d \simeq 2 \times 10^{-4}$. As shown in Table I, the single-crystal and powder results are in agreement within the experimental errors. The reason for the discrepancy between our measured value of the lattice constant of the Exxon crystal and that reported for stoichiometric powders is not clear. Assuming that there is no error in measurement, the discrepancy could be explained if the stoichiometry of the final crystal is lower than that of the starting powder. (Such an interpretation is consistent with our thermopower measurements which will be discussed below.) Thompson *et al.*[2] have reported the c-axis lattice parameter as a function of stoichiometry (x in $Ti_{1+x}S_2$) for powder samples. Using this data, our c-axis lattice parameter for the Exxon sample would correspond to the composition $Ti_{1.005}S_2$. Another possible explanation is that defects which influence the lattice spacing[1,4] are introduced in the single-crystal growth. Because of these uncertainties, we do not believe that it is justified to assign quantitatively a value of nonstoichiometry to our single crystals based on our measured lattice constants and the published data. Instead we will consider the lattice constant as an indicator of the relative nonstoichiometry of the various single crystals. We expect the nonstoichiometry to increase with increasing growth temperature. The resulting excess titanium atoms are expected to be electronic donors, which would increase the carrier concentration.

As shown in Table I, these trends were observed. The smallest lattice parameters and the lowest carrier concentrations were found in crystals grown at the lowest temperatures and with sulfur as the transport agent (batch nos. 164 and 9). The electronic properties (to be discussed in Sec. III) and lattice

parameters of these crystals were virtually identical to those measured in the Exxon highly stoichiometric crystals. The carrier concentration and the *c*-axis lattice parameter increased when iodine transport was used (compare batches 6 and 3). However, iodine doping does not appear to be the source of carriers, since the latter are present in concentrations much larger than the iodine concentration detected in the crystals (about 100 ppm).

III. MEASUREMENTS

A. Electrical properties

The *a*-axis electrical resistivity ρ and the Hall coefficient R_H of the $Ti_{1+x}S_2$ single crystals were measured with the van der Pauw method. All the samples were thin plates cleaved from as-grown crystals with the *c* axis perpendicular to the plate faces. The thickness measured optically ranged between 40 and 150 μm. Low-resistance contacts to the crystals were made with gold paste (Englehard No. A1644). These contacts were found to be stable at temperatures as high as 700 K. Repeated temperature cycling between 77 and 700 K and measurement of ρ and R_H at and below 300 K showed that the properties of the crystals remained unchanged when these gold contacts were employed. In contrast, indium contacts were found to be unstable even at room temperature: After a few hours, a portion of the samples adjacent to the contacts changed color and developed a large number of microcracks, apparently as the result of intercalation by In. Generally, the contacts were made to the plate faces, but experiments where the contacts were made to the sides indicated negligible differences in properties except in the case of the magnetoresistance. The measured resistivity values and Hall coefficient at high and low temperature of crystals from the same batch, but having different thicknesses agreed to within the uncertainty of the thickness measurement. This result indicates that surface-conductivity effects are not important in our resistivity or Hall-coefficient measurements.

Most of the measurements were made in the range 77—700 K using a low-frequency ($\sim$100 Hz) ac current and a dc magnetic field (1—4 kG). Below room temperature, the measurements were carried out in a liquid-nitrogen cryostat; the temperature was measured with a coppper Constantan thermocouple. Data at 4.2 and 77 K were obtained by immersing the samples into the liquid-helium or liquid-nitrogen reservoir. For the measurements above room temperature, the samples were mounted in a quartz cell that was placed in a furnace. The temperature was determined with a platinum resistor and with a type-K thermocouple. Oxidation of the crystals was avoided by continuously flowing helium gas through the quartz cell. The helium gas was first passed through copper mesh at 500 °C in order to remove any oxygen impurities.

Table II shows the *a*-axis resistivity and the Hall coefficient at 300 and 77 K and the 4.2-K resistivity of crystals with different stoichiometries. The carrier concentration calculated from R_H on the basis of a single-carrier model is also shown in Table II. The repeatability in the values of ρ and R_H measured from different samples of the same batch was

TABLE II. Experimental results of resistivity, Hall coefficient and thermoelectric power of $Ti_{1+x}S_2$ single crystals having varying degrees of nonstoichiometry.

Single-crystal batch number	Resistivity ($\mu\Omega$ cm) 4.2 K	77 K	300 K	Hall coefficient (10^{-2} cm^3/C) and carrier concentration (10^{20} cm^{-3}) (in parentheses) 77 K	300 K	Thermoelectric power (μV/K) 300 K
164	165	250	2110	2.5 (2.5)	2.9 (2.2)	240
9	102	190	1950	2.5 (2.5)	2.8 (2.2)	
6	99	170	1500	1.9 (3.3)	2.1 (3.0)	203
7	88	131	805	0.71 (8.8)	0.84 (7.4)	
3	93	135	790	0.75 (8.3)	0.83 (7.5)	131
8	99	134	560	0.46 (14.0)	0.49 (13.0)	101
1	133	156	377	0.17 (37.0)	0.19 (34.0)	56
Exxon	166	270	1990	2.4 (2.6)	2.6 (2.4)	245

good (about 10—15 %). Most of the discrepancies were due to uncertainties in the sample thickness.

The Hall coefficient was found to be independent of the magnetic field in the range of 0—4 kG and negative (electronlike) for all samples. In addition, R_H was essentially independent of temperature between 77 and 300 K, the ratio $R_{H,300}/R_{H,77}$ changing only slightly from about 1.2 for the most stoichiometric crystals to about 1.0 for the least stoichiometric ones. As Table II shows, the values of the resistivity and the Hall coefficient of the highly stoichiometric Exxon crystal are virtually identical to those of our most stoichiometric samples.

For a limited number of samples the measurements were extended to temperatures below 77 K using a ^{4}He cryostat. In these measurements a given TiS_2 sample, mounted on a sapphire support, was thermally anchored to a "one-degree" pot. The pot was isolated from the ^{4}He bath by a stainless-steel pumping line. Temperatures below 4.2 K were attained by pumping on the liquid-helium-filled pot; temperatures above 4.2 K were established by heating the evacuated pot. The sample temperatures were determined using a germanium resistor which was calibrated from 1.5 to 100 K. The measurements were carried out using a 200-Hz ac current of ~ 1.5 mA. The magnetic field was established using a superconducting solenoid. Up to its maximum field (50 kG), the magnet had a linearity of 1%. Owing to the uncertainties in sample thickness, the uncertainty in the absolute values of the resistivity in these measurements is also 10—15 %; however, the error in the relative values of the resistivity is much less ($\sim 0.1\%$).

Figure 1 shows results of the temperature dependence of the a-axis resistivity for crystals with varying degrees of stoichiometry. These results were obtained on two sets of crystals; each set consisted of four single crystals taken from batches 1, 3, 6, and 164. One set was used for the measurements in the ^{4}He cryostat and the other for the measurements in the liquid-N_2 cryostat and the furnace. In Fig. 1 we have plotted the logarithm of the resistivity at temperature T, $\rho(T)$, minus that at $T \sim 0$, $\rho(0)$, as a function of the logarithm of the temperature. For $\rho(0)$, we used the resistivity values at 2 K for the samples measured in the ^{4}He cryostat, and the values at 4.2 K (obtained by immersion in liquid He) for the other samples. In the overlapping temperature region, 77—100 K, only minor discrepancies were found between the absolute values of the resistivities of the two sets of crystals, most likely arising from uncertainties in the thickness of the samples. For the plots of Fig. 1, the data from the ^{4}He cryostat were shifted to coincide with the other data in the overlapping range 77—100 K. The normalization factors for these fits were 0.85, 1.03, 0.78, and 0.88 for samples 164, 6, 3, and 1, respectively. Note that $\rho(T) - \rho(0)$ equals $\rho(0)$ near 100 K. Below 15 K, $\rho(T) - \rho(0)$ is less than 1% of $\rho(0)$ and very sensitive to its precise value. For this reason we have omitted the very-low-temperature data from Fig. 1. It is presented in a different form in Figs. 2(a) and 2(b). It is apparent that the data in Fig. 1 cannot be fitted by a straight line over the entire temperature range from 10 to 700 K. If we restrict, however, this power-law fit to temperatures higher than 70—80 K, we obtain the solid lines of Fig. 1, i.e., the resistivity follows the approximate relationship $\rho(T) - \rho(0) = aT^m$. As shown in Fig. 1, the value of the exponent m increases with increasing stoichiometry from a value of about 1.85 for the least stoichiometric crystals to about 2.2 for the most stoichiometric. Above about 40 K, the absolute values and the temperature dependence of our most stoichiometric crystals are in good agreement with previously published data of Thompson.[7]

Below about 40 K, the data can again be represented by straight lines with slopes near 3 indicating a T^3 temperature dependence. Figures 2(a) and 2(b) show some of the raw resistivity data from the ^{4}He cryostat (including that below 15 K) plotted as a function of T^3. The temperature range of validity of this T^3 power law appears to be somewhat larger for the more stoichiometric samples (nos. 164 and 6).[11]

Hall-effect studies in the ^{4}He cryostat showed that R_H continued to decrease slightly with temperature down to 4 K. Figure 3 shows the carrier concentration n calculated from R_H for samples 164, 6, and 1 in the range 4—100 K. It appears that n decreases roughly linearly with T with a maximum temperature coefficient for sample no. 6 of 0.12%/K. These results are generally in agreement with those obtained at higher temperatures (see, for example, Table II; small differences in the absolute values of R_H between the two sets of data can be rationalized in terms of uncertainties in sample thickness).

The magnetoresistance was also measured as a function of magnetic field between 0 and 50 kG for a series of different temperatures. The data at 5 K for samples 1, 6, and 164 are shown in solid lines in Figure 4. The contacts for all samples except 164b were on the edges of the crystal. For 164b they were on the top surface. Measurements as high as

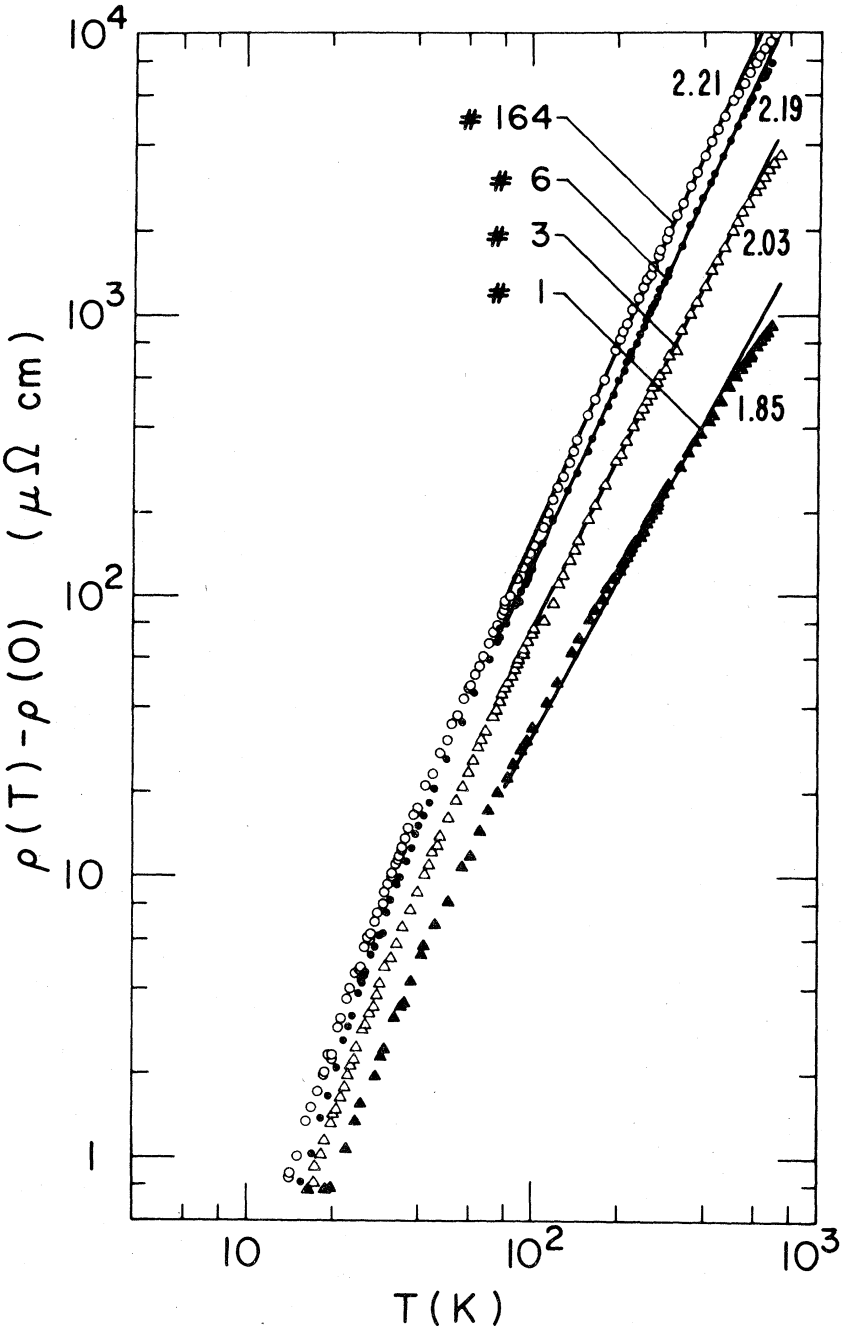

FIG. 1. Log-log plot of the temperature-dependent electrical resistivity of four samples of titanium disulfide $Ti_{1+x}S_2$ with varying degrees of nonstoichiometry. Below about 40 K the resistivity of all samples varies approximately as T^3. Above 100 K, the resistivity varies as T^y where $y = 2.21$ for the most stoichiometric sample (no. 164) and $y = 1.85$ for the least stoichiometric (no. 1). Note that this temperature dependence continues well above the Debye temperature of 235 K. The corresponding carrier concentrations are given in Table II.

80 K gave similar results, that is, to a first approximation the magnetoresistance effects are independent of temperature. The comparatively large magnetoresistance in sample no. 6 does not seem to correlate with other properties of this crystal. The difference between the graphs for 164 and 164b suggests that the nature of the contacts might be involved. We therefore present the results at this stage

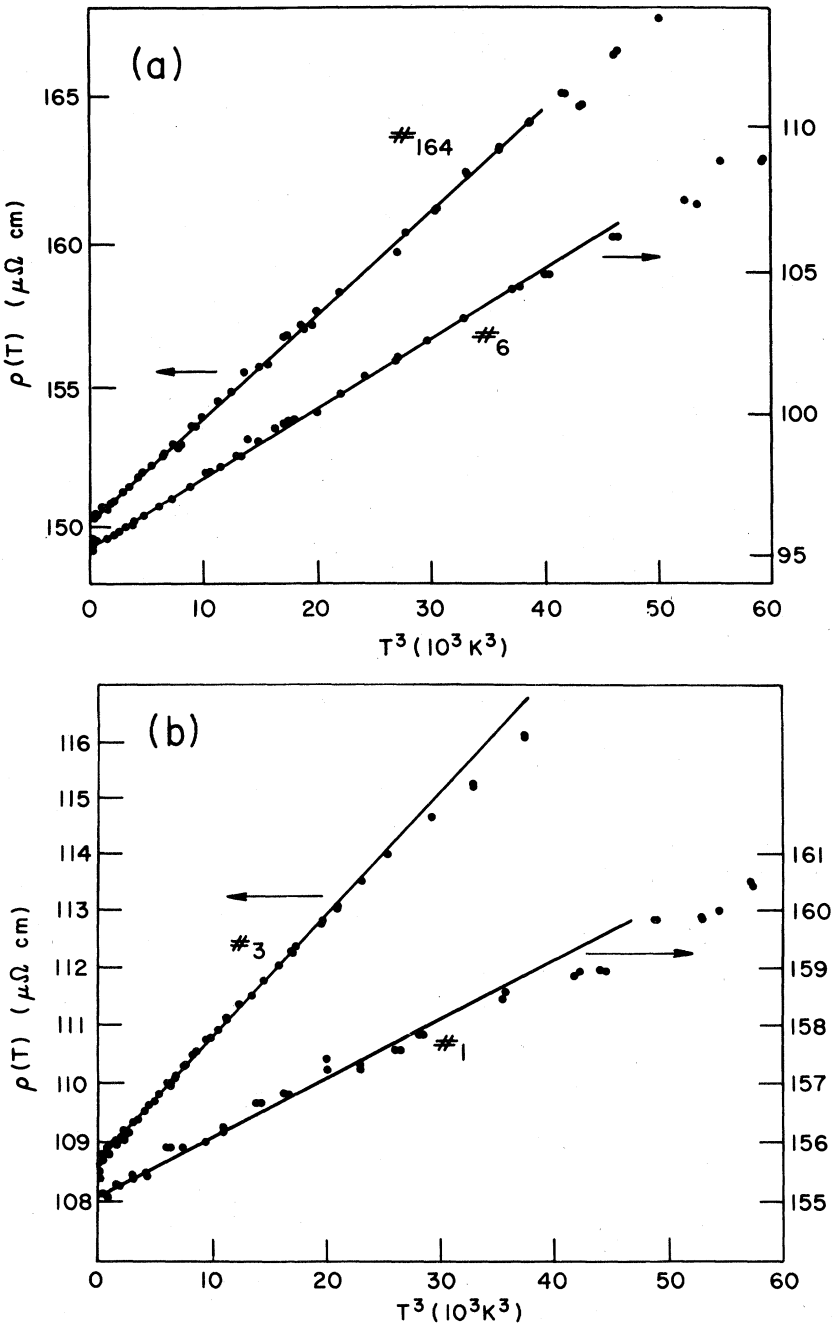

FIG. 2. Low-temperature resistivity of four samples of titantium disulfide with varying degrees of nonstoichiometry plotted against T^3. Below about 40 K, the data can be fitted with straight lines indicating a $\rho(T) = \rho(0) + cT^3$ relationship in this temperature range.

for completeness and caution against drawing any strong conclusions from these preliminary data.

For the measurement of the thermoelectric power, the two ends of a crystal were pressed against two copper blocks and a series of temperature differences ΔT were established between the blocks by means of heaters. Constantan wires were attached to the copper blocks to form thermocouples for the measurement of the temperatures. Plots of the measured thermovoltage of the samples versus ΔT gave straight lines passing through the origin. The thermoelectric power S was determined from the slope of such a line after correcting for the thermoelectric power of copper, $S(\mathrm{Cu}) = 1.7\ \mu\mathrm{V/K}$.

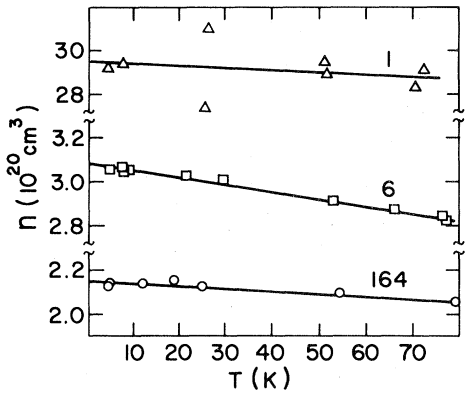

FIG. 3. Temperature dependence of the carrier concentration n calculated from the Hall coefficient R_H in the range 0—80 K for some titanium disulfide samples with varying degrees of nonstoichiometry. n decreases approximately linearly with increasing T ($n \simeq n_0 - cT$).

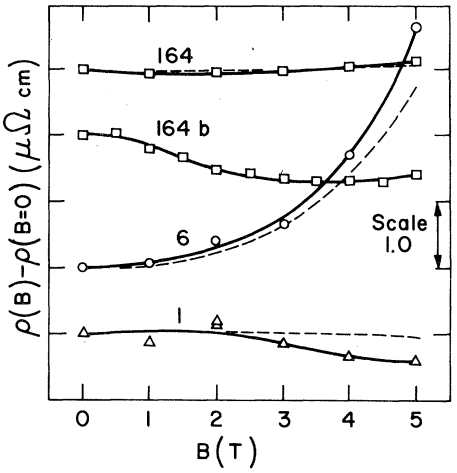

FIG. 4. Magnetic field dependence of the magnetoresistance of some titanium disulfide samples with varying degrees of nonstoichiometry. The solid lines and data points represent data obtained at 5 K. The dotted lines represent data obtained at 80 K.

The values of S at 300 K for various crystals are shown in Table II. The sign of S was found to be negative for all crystals, indicating that the majority carriers are electrons. Again, our most stoichiometric crystals (sample no. 164) and the Exxon materials have almost identical values of thermoelectric power.

B. Reflectivity

The room-temperature reflectivity of several $Ti_{1+x}S_2$ single crystals was measured with a Perkin-Elmer infrared spectrometer (IR 521). The absolute value of the reflectivity was determined by using a germanium crystal and an aluminum mirror as references.

Figure 5 shows the 300-K reflectivity spectra of freshly cleaved $Ti_{1+x}S_2$ crystals. The shapes of the spectra strongly suggest free-carrier absorption: Each spectrum shows a well-defined plasma edge

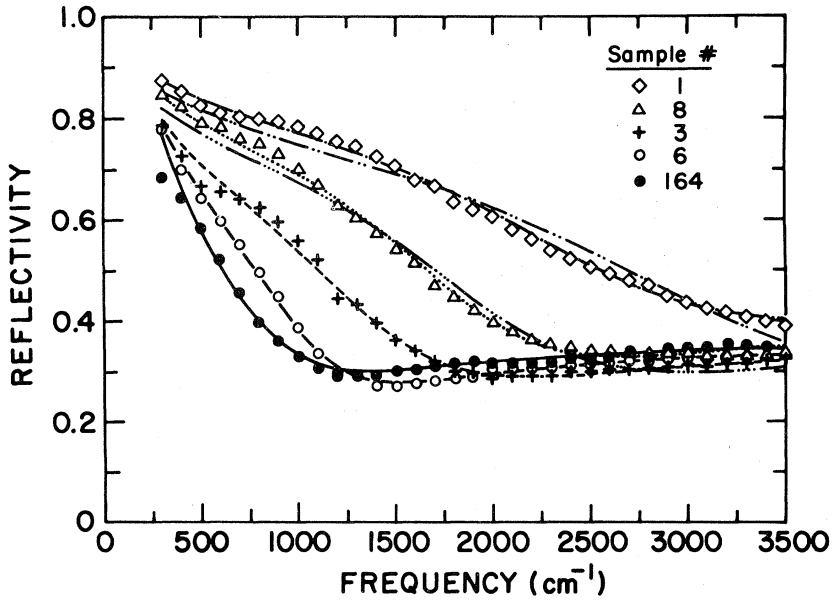

FIG. 5. Infrared reflectivity at room temperature of freshly cleaved single crystals of titanium disulfide with various degrees of nonstoichiometry. The plasma edge shifts to higher energy as the crystals become more nonstoichiometric. The curves are free-carrier Drude fits to the data, for samples 1 and 8 both three- and two-parameter fits are shown. The other curves are all three-parameter fits. The resulting plasma frequency may be obtained from Table III. Data are shown for samples 1 (◇), 8 (△), 3 (+), 6 (○), and 164 (●).

that shifts to higher frequencies with increasing degree of nonstoichiometry. We find that we can fit the data for all samples with a single-carrier Drude formula for reflectivity,

$$R = \frac{(N-1)^2 + K^2}{(N+1)^2 + K^2} ,$$

where

$$N = \frac{1}{\sqrt{2}}[(\epsilon_1^2 + \epsilon_2^2)^{1/2} + \epsilon_1]^{1/2}$$

and

$$K = \frac{1}{\sqrt{2}}[(\epsilon_1^2 + \epsilon_2^2)^{1/2} - \epsilon_1]^{1/2} ,$$

and where

$$\epsilon_1 = \epsilon_\infty - \frac{\omega_p^2 \tau_{\text{opt}}^2}{1 + \omega^2 \tau_{\text{opt}}^2} ,$$

$$\epsilon_2 = \frac{\omega_p^2 \tau_{\text{opt}}^2}{\omega(1 - \omega^2 \tau_{\text{opt}}^2)} ,$$

with

$$\omega_p^2 = \frac{4\pi e^2 n}{m_{\text{opt}}} .$$

In these expressions, n_{ω_p} is the carrier concentration, ω_p the plasma frequency, τ_{opt} the optical relaxation time, m_{opt} the optical mass, ϵ_∞ the high-frequency dielectric constant, and ϵ_1 the real part and ϵ_2 the imaginary part of the dielectric constant.

The three-parameter (ϵ_∞, ω_p, and τ_{opt}) nonlinear least-squares fits to the experimental data for the various samples are shown by the curves in Fig. 5. The values of the Drude parameters are given in Table III. The uncertainty in the derived values of the Drude parameters was determined by examining the sensitivity of these parameters to the extreme of possible experimental error ($\pm 5\%$). First the experimental data was multiplied by 0.95 and 1.05, and Drude fits were performed on these modified data. A similar analysis was performed on the data modified by the addition or subtraction of a constant value corresponding to 5% of the average reflectivity. The maximum uncertainty in n_{ω_p} and $1/\tau_{\text{opt}}$ ranges between 3% and 14% for n_{ω_p} and 11% and 20% for $1/\tau_{\text{opt}}$ and are shown in Figs. 7 and 10.

The Drude fits to the data are adequate, but the calculated values of ϵ_∞ for the two least stoichiometric samples (nos. 8 and 1) appear to be too large. To check the sensitivity of our fit to the value of ϵ_∞, we have constrained ϵ_∞ to be 18 and fitted the data by varying only ω_p and τ_{opt}. These two-parameter fits are also shown in Fig. 5 and the resulting Drude parameters are given in parentheses in Table III. The apparent carrier concentration, $n_{\omega_p} = m_e \omega_p^2 / 4\pi e^2$, is defined using the free-electron mass and differs from the actual carrier concentration by the ratio m_{opt}/m_e. The values of n_{ω_p} determined by the two-parameter fit is within 10% of the value from the three-parameter fit and $1/\tau_{\text{opt}}$ is within 15%. This difference will not affect our overall conclusions. Lucovsky *et al.*[12–14] also had difficulty in fitting the reflectivity of a highly nonstoichiometric sample to a single-carrier Drude formula. This difficulty may arise because the plasma edge in the nonstoichiometric samples is approaching an interband transition (direct gap[15] 0.8 eV).

The sample measured by Benda[16] at 4.2 K has a plasma frequency close to that of sample no. 3, but he found the optical scattering rate $1/\tau_{\text{opt}}$ to be 3–4 times smaller. This difference could be due to the lower temperature of his measurement.

In addition to freshly cleaved crystals, the reflectivity spectra from as-grown surfaces were also investigated. Figure 6 compares the spectra from as-grown and freshly cleaved surfaces for the most stoichiometric (sample no. 164) and the least stoichiometric (sample no. 1) crystals. We find that for the least stoichiometric crystals, the plasma edge of the freshly cleaved surface is substantially shifted to higher frequencies relative to the plasma edge of the as-grown surface. However, for the most stoichiometric crystals we find that the shift is considerably smaller and in the opposite direction. In fact, we find that the plasma frequency of an as-grown surface is nearly the same for all crystals.

The optical scattering rates for the as-grown surfaces of the nonstoichiometric samples are 2–3 times smaller than the rates of freshly cleaved surfaces. Both the plasma frequency and the scattering rate of the as-grown surfaces of nonstoichiometric samples are similar to those measured for the freshly cleaved surfaces of more nearly stoichiometric samples (e.g., no. 6). This indicates that the surface layer may be more stoichiometric than the bulk in these samples. The size of this surface layer has not been investigated directly, but bulk spectra are obtained by removing approximately 5–10 μm from the surface of our as-grown samples which are typically 40 to 100 μm thick. Lucovsky[17] has observed similar differences between as-grown and freshly cleaved surfaces, and he suggested that the surface layer may be grown during the cooling from the growth temperature to ambient. Nonstoichiometric

TABLE III. Drude parameters derived from room-temperature reflectivity data of $Ti_{1+x}S_2$ single crystals having varying degrees of nonstoichiometry. n_{ω_p} is defined using the bare electron mass. Therefore it differs from the actual electron concentration by the ratio m_{opt}/m_e. The values in parentheses for crystals nos. 8 and 1 were obtained with a two-parameter fit assuming $\epsilon_\infty = 18$.

Single-crystal batch number	n_{Hall} (10^{20} cm^{-3})	Cleaved crystal surface n_{ω_p} (10^{20} cm^{-3})	$1/\tau_{opt}$ (10^{14} s^{-1})	ϵ_∞
164	2.2	1.9	2.4	16.1
9	2.2			
6	3.0	2.8	2.0	18.3
3	7.5	5.1	2.9	16.2
7	7.4			
8	13.0	11.0	3.9	22
		(11.0)	(3.4)	(18)
1	34.0	30.0	4.3	31
		(27.0)	(5.0)	(18)
Exxon	2.4	2.2	2.9	16.4

Single-crystal batch number	As-grown crystal surface n_{ω_p} (10^{20} cm^{-3})	$1/\tau_{opt}$ (10^{14} s^{-1})	ϵ_∞
164	2.6	2.6	15.9
3	3.0	1.4	18.1
1	3.4	1.8	14.6

crystals are grown at higher temperatures (and resulting sulfur pressures) than the stoichiometric samples. During cooling the temperature passes through the growth temperature for stoichiometric TiS_2 (625 °C). If the last few layers were transported at this temperature, the surface layer would be highly stoichiometric and one would expect to find similar surface layers for all nonstoichiometric samples.

IV. DISCUSSION

A. The semiconducting nature of TiS_2

In this section we consider the basic question of whether titanium disulfide is a semimetal or a semiconductor and analyze our optical and electrical transport data to determine what evidence they provide in support of one or the other model. Because all these different measurements were carried out on each crystal (or crystals from the same batch) we have been able to establish strong correlations between various properties that provide convincing evidence that TiS_2 is a semiconductor.

Our analysis is based on the following expressions for the conductivity σ, Hall coefficient R_H, and thermoelectric power S of a two-carrier system[18]:

$$\sigma = e(n_1\mu_1 + n_2\mu_2) \ , \tag{1}$$

$$R_H = \frac{-1}{e}\frac{n_1 e_1 \mu_1^2 + n_2 e_2 \mu_2^2}{(n_1\mu_1 + n_2\mu_2)^2} \ , \tag{2}$$

$$S = \frac{-A\pi^2 k_B^2 T}{3e}\frac{n_1 e_1 \mu_1/E_{F_1} + n_2 e_2 \mu_2/E_{F_2}}{n_1\mu_1 + n_2\mu_2} \ . \tag{3}$$

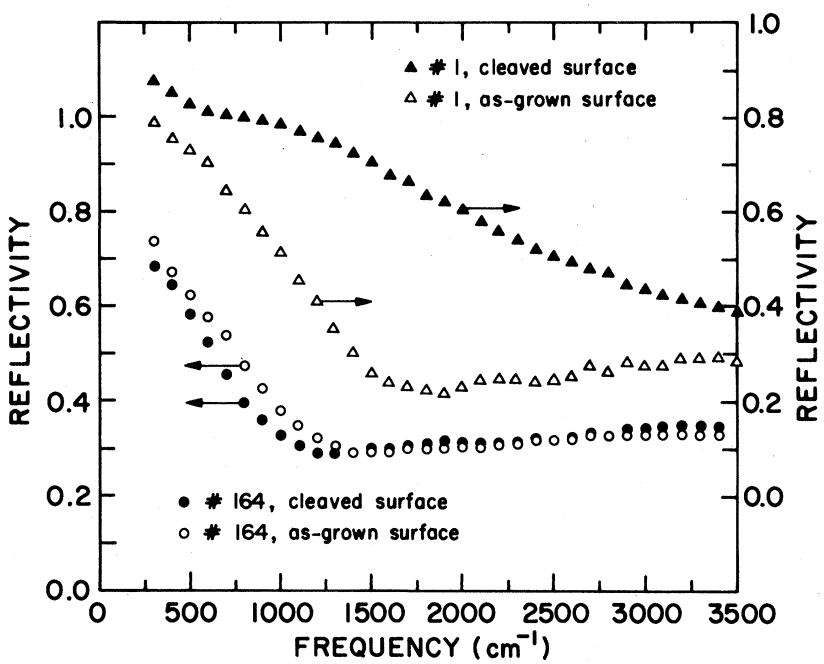

FIG. 6. Infrared reflectivity of freshly cleaved and as-grown surfaces of titanium disulfide. For the most stoichiometric sample (no. 164), there is little difference between the as-grown surface and the freshly cleaved bulk surface. For the least stoichiometric sample (no. 1), the plasma edge of the freshly cleaved surface is substantially shifted to higher frequencies relative to the plasma edge of the as-grown surface. The plasma frequency of an as-grown surface is nearly the same for all crystals measured.

E_{F_i}, n_i, μ_i are the Fermi energy, concentration, and mobility of the ith carrier, respectively. The mobility is given by

$$\mu_i = \frac{e\tau_i}{m_i} \quad , \tag{4}$$

where m_i is the effective mass and τ_i is the relaxation time. For a semimetal $e_1 = -e_2 = 1$ and for a system with two different types of electrons (e.g., an s-d metal) $e_1 = e_2 = 1$. The factor A in Eq. (3) depends on the scattering mechanism; for a free-electron gas, $A = 1$ for impurity scattering and $A = 3$ for phonon scattering at high temperatures. We note that Eqs. (1)–(3) reduce to single-carrier expressions by letting n_2 go to zero.

The expressions above are valid only when the interactions between the two types of carriers are negligible. The case of interacting carriers has been discussed by Kukkonen and Maldague,[19,20] who have derived expressions for σ and R_H for a number of systems. For an interacting electron-hole system (semimetal) they find the following results that are relevant to the present analysis: (1) The Hall coefficient of an uncompensated semimetal ($n \neq p$) is temperature dependent and (2) the Hall coefficient of an uncompensated semimetal is larger than that of a compensated semimetal ($n = p$) at room temperature. These theoretical predictions are not observed in our experiments; we find that R_H is nearly independent of temperature in the range 4–300 K for all samples and that R_H decreases as the nonstoichiometry of the samples increases. These experimental results therefore show that electron-hole interactions are not dominant in TiS_2 and provide justification for considering only noninteracting carriers in the semimetallic model. The theory predicts that strong interactions will not have such a dramatic effect in a semiconductor and the experimental results do not rule out strong electron-electron interactions in this case. We will continue with the analysis based on noninteracting electrons and abandon it only if faced with a contradiction.

In Sec. III, we found that the reflectivity data for all crystals can be fitted adequately with a single-carrier Drude expression (the carrier concentrations obtained from this analysis are shown in Table III). This result, however, does not eliminate a two-carrier system, because a two-carrier Drude expression is equivalent to that of a single carrier if the two carriers have the same optical scattering time

τ_{opt}. The plasma frequency, in this case, is given by

$$\omega_p^2 = 4\pi e^2 \left[\frac{n_1}{m_{\text{opt},1}} + \frac{n_2}{m_{\text{opt},2}} \right] . \quad (5)$$

Let us next consider the Hall-effect data. The experimental result that R_H is essentially independent of temperature for all samples is consistent with a single-carrier system with carrier concentrations independent of temperature, i.e., without carrier freeze-out. The carrier concentrations calculated from R_H on the basis of a single-carrier model are given in Table II. The lack of temperature dependence of R_H, however, is also consistent with a two-carrier system. For example, Eq. (2) predicts a temperature-independent R_H when n_1, n_2, and the ratio μ_1/μ_2 are temperature independent, or when $n_2\mu_2 << n_1\mu_1$ and n_1 is independent of temperature. Therefore consideration of the Hall data alone or the optical data alone cannot distinguish between one- and two-carrier systems. The conclusion is quite different when we combine the Hall effect and the optical data together.

For a single-carrier system, the carrier concentrations deduced from the plasma frequency and from the Hall coefficient are related by $n_{\text{Hall}} = (m_{\text{opt}}/m_e)n_{\omega_p}$. Figure 7 shows a plot of n_{Hall} against n_{ω_p}. The data fall on a straight line with a slope of 1.3. These results are thus consistent with a single-carrier model with a constant optical mass (i.e., independent of band filling) equal to $1.3m_e$. For a two-carrier model, the ratio of $n_{\text{Hall}}/n_{\omega_p}$ is is given by

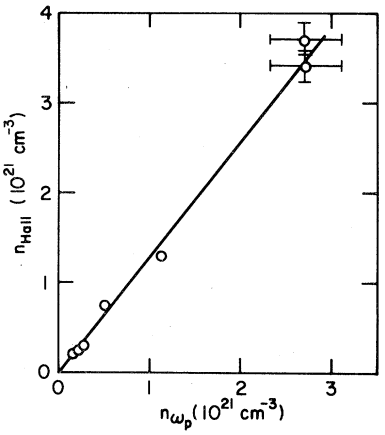

FIG. 7. Carrier concentration deduced from the Hall coefficient plotted against that deduced from the plasma frequency. This is equivalent to plotting the experimentally observed inverse Hall coefficient against the square of the plasma frequency. The straight-line behavior is consistent with a single-carrier model and inconsistent with a semimetal. The slope yields the optical mass $m_{\text{opt}}/m_e = 1.3$. Two additional data points not mentioned elsewhere are included in the figure.

$$\frac{n_{\text{Hall}}}{n_{\omega_p}} = \frac{4\pi e}{R_H\omega_p^2 m_e} = \frac{m_{\text{opt},1}}{m_e} \frac{[1 + (n_2/n_1)(\mu_2/\mu_1)]^2}{[1 \pm (n_2/n_1)(\mu_2^2/\mu_1^2)][1 + (n_2/n_1)(m_{\text{opt},1}/m_{\text{opt},2})]} , \quad (6)$$

where the plus sign is for a semiconductor and the minus for a semimetal. Experimentally this ratio is 1.3, independent of the value of ω_p or R_H. If we continue to assume that the differences among our samples are due to differences in nonstoichiometry and carrier concentration, the experimental results of Fig. 7 require that $n_{\text{Hall}}/n_{\omega_p}$ remain constant as n_1 and n_2 vary. For the purpose of determining the implications of this constraint, we make the assumption that $m_{\text{opt},1}$ and $m_{\text{opt},2}$ are independent of n_1 and n_2. The mobilities, however, are likely to depend on carrier concentrations. The scattering rate may be written as $1/\tau \propto \langle M^2 \rangle \rho(E_F)$, where $\rho(E_F)$ is the density of states at the Fermi level and $\langle M^2 \rangle$ is an average of the square of the scattering matrix element. If $\langle M^2 \rangle$ is a constant, $1/\tau$ will be proportional to $\rho(E_F)$ which varies as $n^{1/3}$ in the simplest approximation. In simple theoretical models $1/\tau$ is proportional to some power of the carrier concentration; therefore the mobility ratio μ_2/μ_1 would be proportional to some power of n_2/n_1. Under these conditions, $n_{\text{Hall}}/n_{\omega_p}$ depends only on the ratio n_2/n_1 and would remain constant as n_1 and n_2 vary only if their variation were such as to keep the ratio n_2/n_1 constant. This, however, cannot occur in the case of a semimetal because an increase in the electron concentration in the conduction band must be accompanied by a decrease in the hole concentration in the valence band. Because the ratio $n_{\text{Hall}}/n_{\omega_p} = 1.3$ remains constant as n_{Hall} and n_{ω_p} each vary by more than a factor of 15, we conclude that titanium disulfide is not a semimetal but a semiconductor.

Although we have ruled out the possibility that TiS_2 is a semimetal, we must still consider whether we are dealing with one or two kinds of electrons, i.e., whether the electrons reside in one or more (nonequivalent) conduction bands (e.g., band

minimum at the L and M points of the Brillouin zone as suggested by band-structure calculations). If we consider again the ratio n_2/n_1, we find that for a two-conduction-band system this ratio does not remain constant as the total electron concentration increases except in the special case where the bottoms of the two types of nonequivalent bands coincide. In this case, $n_2/n_1 = (m_2/m_1)^{3/2}$. Similarly, Eq. (3) shows that the experimentally observed $S \propto n^{-2/3}$ dependence cannot be valid unless $E_{F_1} = E_{F_2}$, i.e., when again the bottoms of the two types of band coincide. Let us examine this case a little further. If $m_2 >> m_1$, the Hall coefficient would correspond to the light carriers and would give a carrier concentration appreciably smaller than the total carrier concentration. This, however, does not appear valid because the analysis in Sec. IV B will show that the carrier concentrations determined from R_H can be accounted for by the amount of nonstoichiometry x (except for $x < 0.005$).

Our data are consistent with a simple single-carrier model and we see no evidence for two inequivalent types of electrons. Further support for this conclusion is provided by an analysis of thermoelectric power data. Figure 8 shows a plot of the measured thermoelectric power S as a function of n_{Hall} for our single crystals. The solid line is a plot of S calculated from Eq. (3) assuming $n_2 = 0$, $A = 3$, and $m_1 = m_e$. The Fermi energy was calculated from $k_F^3 = 3\pi^2 n_{\text{Hall}}/3$ under the assumption that the electrons reside in three equivalent spheres centered on the faces of the hexagonal Brillouin zone of TiS_2. The comparison in Fig. 8 suggests that the experimental data can be described approximately by a single-carrier free-electron model with m_1/m_e of the order of unity. This result agrees with our previous determination that $m_{\text{opt}}/m_e = 1.3$. Note that the agreement between experiment and simple theory is best for the least stoichiometric crystals. The discussion of the temperature data is continued below.

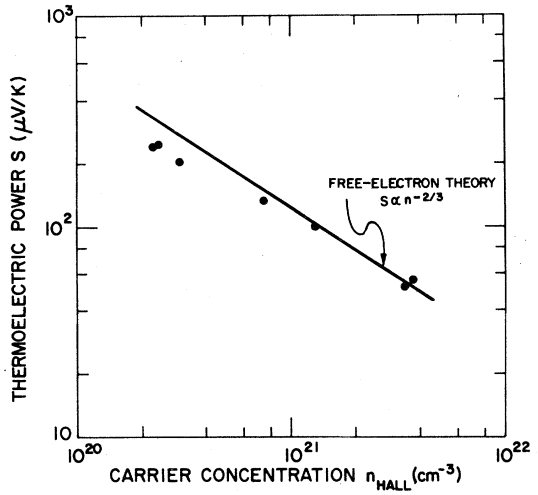

FIG. 8. Thermoelectric power at 300 K plotted against the carrier concentration deduced from the Hall coefficient. The solid line is the prediction of the single-carrier free-electron model described in the text.

B. The source of the carriers

In Sec. IV A, we showed that our measurements establish that titanium disulfide is not a semimetal but a degenerate semiconductor. In this case, it is of considerable interest to determine the origin of these extrinsic electrons, especially in view of the fact that we, as others in past studies, were not able to obtain materials with $n < 2 \times 10^{20}$ cm^3.

The high purity of initial materials and the results of impurity analysis of grown crystals show that impurities are not the source of the carriers in our samples, even in those with the lowest carrier concentrations. The next possibility to consider is nonstoichiometry. The results of a number of previous studies[1,2,4] suggest that the excess Ti atoms in $Ti_{1+x}S_2$ reside in the interlayer van der Waals sites and act as donors. The number of electrons contributed by each donor to the conduction band is expected to be four, although a larger number has been suggested by Wilson.[4] A direct determination of x by chemical methods, although highly desirable, was not attempted in our studies, because of the unavailability of a sufficient quantity of single-crystal materials. An indirect method for determining the values of x in our crystals would be to use our measured c-axis lattice parameters in conjunction with the published data[2] on the relationship between x and the lattice constant of powder samples of $Ti_{1+x}S_2$. This approach was discounted, however, because of the uncertainties in the measured and published values of the lattice constant as discussed in Sec. II. Another indirect method is based on thermoelectric power data. Thompson *et al.*[2] have measured the dependence of the room-temperature thermoelectric power of pressed powders of $Ti_{1+x}S_2$ on the value of x. These results are reproduced in Fig. 9 and can be used to infer the value of x in our crystals from the measured value of the thermoelectric power. To check the validity of this method and the overall consistency of our electrical and optical data, we also proceeded

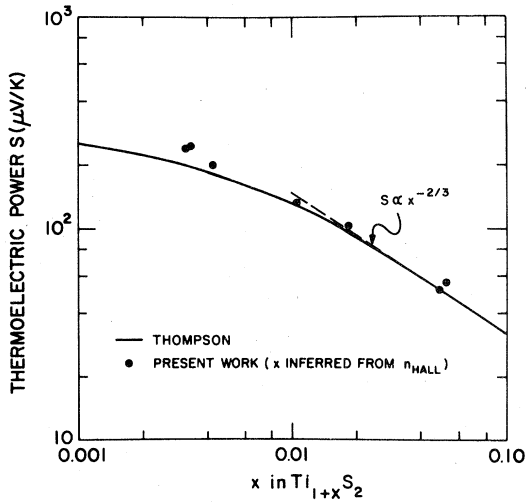

FIG. 9. Thermoelectric power at 300 K plotted against the nonstoichiometry x of $Ti_{1+x}S_2$ crystals. The values of x were calculated from the carrier concentration n_{Hall} assuming that the carriers arise from excess titanium and each titanium atom contributes four electrons. The solid line reproduces the data of Thompson *et al.* (Ref. 2) who measured S and x of $Ti_{1+x}S_2$ powders. The dotted line represents the $S \propto n^{-2/3}$ or $x^{-2/3}$ predictions of a single-carrier free-electron model.

to calculate x from the measured values of n_{Hall}. For the purpose of making a comparison, we assume that all the electrons arise from excess titanium and that each Ti atom contributes four electrons to the conduction band. We can then calculate x using the expression $x = n_{\text{Hall}}/[4(1.75 \times 10^{22})]$ where 1.75×10^{22} is the number of Ti atoms in TiS_2 per cm^3. The values of x calculated in this manner were then used in Fig. 9 to plot our thermoelectric power data against x. The agreement between our data and those of Thompson *et al.*[2] is excellent for large x ($x > 0.01$). In addition, as shown in Fig. 9, these data at large x follow an $S \propto x^{-2/3}$ relationship, in agreement with the single-carrier free-electron model. These results strongly suggest that, for $x \geq 0.01$, the source of the carriers are excess Ti atoms, each contributing four electrons to the conduction band. The agreement between the two sets of data becomes less satisfactory for low x. For example, on the basis of the data of Thompson *et al.*, our most stoichiometric crystals (sample no. 164) with $S = -240\ \mu V/K$ should have $x = 0.001$; according to our analysis based on n_{Hall}, however, x should be 0.003. (We note that for the Exxon highly stoichiometric crystals we obtained $S = -245\ \mu V/K$ and $n_{\text{Hall}} = 2.3 \times 10^{20}$ cm^{-3}, values that are virtually identical to those obtained with our best crystals. As with the lattice constants, we again obtain evidence that the nonstoichiometry of the Exxon crystals is larger than that of the starting powder.) The reason for the discrepancy between the two calculated values of x for our most stoichiometric cyrstals is not clear. One possibility is that the carriers still arise from some small residual nonstoichiometry and some small error has been made in the determination of S or x (especially when x is less than 0.005). Another possibility is that for low x each excess Ti contributes more than four electrons; as mentioned previously, this has been suggested by Wilson,[4] but is not supported by any other evidence. A third possibility is that our samples contain about 1.5×10^{20} electrons per cm^3 which do not arise from excess titanium, so that the total carrier concentration is given by $n = 1.5 \times 10^{20} + [4(1.75 \times 10^{22})]x$. These residual carriers dominate at low x but make a negligible contribution to the total carrier concentration at $x > 0.01$. A possible source of these residual electrons, if they indeed exist, is the so-called "displacement defects." On the basis of x-ray diffraction line-intensity analysis, Takeuchi and Katsuta[1] have suggested that, at low x, some of the Ti atoms move into van der Waals gap sites leaving behind Ti vacancies. Further support for the existence of these defects is provided by the anomalies of the lattice constant of $Ti_{1+x}S_2$ at low x.[1,2] The concentration of the displacement defects increases with increasing temperature and can be substantial. For example, Takeuchi and Katsuta[1] estimate that in their crystals grown at about 1000 °C, as x tends to zero, between 2.5% and 3% of the Ti ions are displaced in the van der Waals gap sites. In spite of the presence of the displacement defects, simple semiconductor physics arguments would still suggest that stoichiometric TiS_2 is not an extrinsic semiconductor but a compensated one, since Ti interstitials and Ti vacancies would be expected to behave as donors and acceptors. These simple arguments, however, are not necessarily valid because vacancies and interstitials, unlike substitutional ions, constitute major lattice perturbations. Wilson[4] has suggested that, in this case, a number of sulfur p-band states (corresponding to the "excess" sulfur created by the displacement defects) are shifted to energies higher than the Fermi level thus eliminating the otherwise acceptor states. These ideas are similar to those developed in detail by Parada and Pratt[21] in their theoretical discussion of cation and anion vacancies and interstitials in PbTe and other IV-VI compounds. (Their theory also provides an interesting explanation for

the absence of freeze-out of extrinsic carriers in these materials.) Because of the basic questions involved in the discussion of the source of the carriers in stoichiometric TiS_2, it appears very desirable to determine x directly on single crystals where the carrier concentration is also obtained from Hall-effect measurements.

C. Scattering mechanism in $Ti_{1+x}S_2$

Acoustic-phonon scattering is the source of the temperature dependence of the resistivity in ordinary metals. Simple acoustic-phonon scattering yields a T^5 resistivity at low T and a linear temperature dependence above about $\theta_D/3$, where θ_D is the Debye temperature (235 K for TiS_2). In contrast, the resistivity of TiS_2 (Figs. 1 and 2) varies as T^3 at low T and as T^y at high T where y varies between 1.85 and 2.2 depending on stoichiometry. (The resistivity of sample no. 164 varies more slowly at temperatures above 500 K. This may be because of its low Fermi temperature $T_F = 760$ K. For sample no. 1, with $T_F = 4480$ K, the power law continues up to the highest temperature.)

Our reflectivity measurements are consistent with our transport data in that the optical scattering rate $1/\tau_{\rm opt}$ obtained from the reflectivity correlates well with the scattering rate $1/\tau_{\rm dc}$ deduced using the room-temperature resistivity and Hall coefficient. This correlation is exhibited in Fig. 10 where $1/\tau_{\rm opt}$ is plotted against $1/\tau_{\rm dc}$. The data are consistent with the linear relationship

$$1/\tau_{\rm opt} = 1/\tau_{\rm dc} + 1.2 \times 10^{14}\,\text{sec}^{-1} \ .$$

Note that $1/\tau_{\rm opt}$ is greater than $1/\tau_{\rm dc}$. This relation is consistent with the increased phase space for optical transitions.

To try to identify the scattering mechanisms we examine the electron mobility at a given temperature as a function of the carrier concentration. The total mobility μ is related to conductivity by

$$\sigma = \frac{ne^2\tau}{m} = ne\mu \ .$$

We consider the mobility rather than the conductivity or resistivity because it is more reliable when comparing measurements made on different samples. In the Van der Pauw technique, the calculated absolute values of both the resistivity and the Hall coefficient are linearly proportional to the thickness of the planar sample. The mobility, however, is given by the ratio of R_H to ρ and is independent of the sample thickness:

$$\mu = \frac{R_H}{\rho} \ .$$

Just as the resistivity is given by the sum of a temperature-dependent and a temperature-independent term, it is convenient to define the corresponding partial mobilities

$$\mu(4.2\ \text{K}) = R_H/\rho(4.2\ \text{K})$$

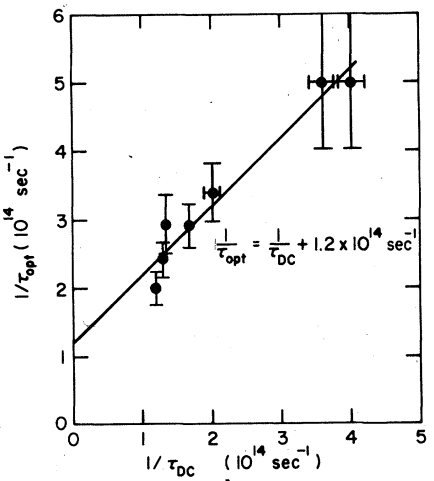

FIG. 10. Optical scattering rate plotted versus the dc scattering rate obtained from the electrical resistivity. The close correlation indicates the consistency of the data. The larger optical scattering rate is consistent with the increased phase space for optical transitions.

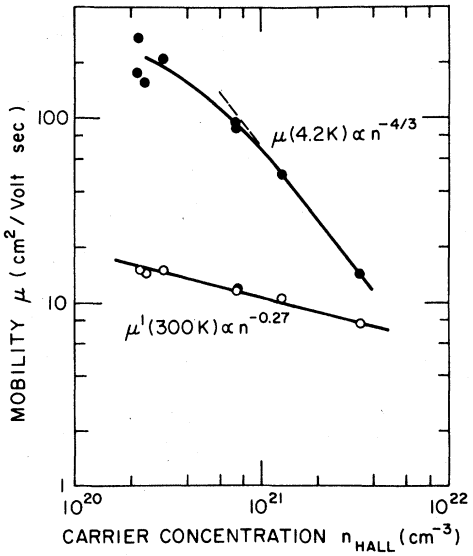

FIG. 11. Carrier concentration dependence of the mobility at 4.2 K and the partial mobility $\mu^1(T) = R_H/[\rho(T) - \rho(4.2\ \text{K})]$ at 300 K.

and

$$\mu^1(T) = R_H/[\rho(T) - \rho(4.2\ \text{K})] \ .$$

$\mu(4.2\ \text{K})$ and $\mu^1(300\ \text{K})$ are plotted against the carrier concentration n in Figure 11.

First consider $\mu(4.2\ \text{K})$ which arises from temperature-independent "impurity" scattering mechanisms. At carrier concentrations above $2 \times 10^{20}/\text{cm}^3$ $\mu(0)$ varies as $n^{-4/3}$. At lower concentrations there is more scatter in the data, but it appears that $\mu(4.2\ \text{K})$ varies more slowly with density. The $n^{-4/3}$ dependence may be understood by the simple argument

$$1/\tau_{\text{imp}} = N_{\text{imp}}\langle M^2\rangle\rho(E_f) \ ,$$

where N_{imp} is the density of impurities, M is the matrix element, and $\rho(E_F)$ is the density of final states. The experimentally observed relationship $\mu = e\tau/m \propto n^{-4/3}$ is obtained if M is independent of n, if $\rho(E_f)$ is given by the free-electron relation $\rho(E_f) \propto n^{1/3}$, and if the scattering impurities are also the source of the electrons, $n \propto N_{\text{imp}}$.

This last condition is also consistent with our earlier conclusion as to the source of the conduction electrons (except for $\sim 1.5 \times 10^{20}/\text{cm}^3$ residual electrons).

Figure 11 shows that the room-temperature partial mobility, $\mu^1(300\ \text{K})$, arising from the temperature-dependent scattering mechanisms, varies as $n^{-0.27}$ over the entire density range. Equivalently $\rho(300\ \text{K}) - \rho(4.2\ \text{K})$ varies as $n^{0.73}$ (see also Ref. 22). Thompson[7] previously reported that $\rho(300\ \text{K}) - \rho(4.2\ \text{K})$ in $Ti_{1+x}S_2$ varied as $n^{-5/3}$. (This corresponds to an $n^{2/3}$ dependence of the mobility.) This $n^{-5/3}$ dependence together with the pure T^2 temperature dependence from 10 to 450 K reported by Thompson led him to conclude that the scattering mechanism was electron-electron scattering (or electron-hole scattering since Thompson also concluded that TiS_2 was a semimetal). Our data conflict with Thompson's. For our most stoichiometric samples ρ varies as T^3 at low T and as $T^{2.2}$ at high T, and we find $\rho(300\ \text{K}) - \rho(4.2\ \text{K})$ varies as $n^{-0.73}$, not as $n^{-5/3}$. Possible reasons for these discrepancies are discussed below.

Although Thompson only published a pure T^2 resistivity, he did observe that the exponent was mildly sample dependent, reaching 2.1 for samples with the highest resistivity ratios $\rho(300\ \text{K})/\rho$ (4.2 K) = 12. Our sample no. 164 has a resistance ratio of 12.8, and the high-temperature resistivity varies as $T^{2.21}$. Our less stoichiometric sample no. 3, $\rho(300\ \text{K})/\rho(4.2\ \text{K}) = 8.6$, showed a $T^{2.03}$ resistivity at high T (see Fig. 1). Therefore our high-temperature data are roughly consistent with Thompson's observations. Our measurements differ more from Thompson's at low T. He reported that the T^2 term continued at least down to 10 K, while all our samples show an approximate T^3 behavior at low T. Since $\rho(T) - \rho(0)$ is less than 10% of $\rho(0)$ below 40 K, $\rho(T)$ must be measured with relative precision of better than 0.5% to be able to establish the power law with confidence. Our relative precision in ρ was about 0.1%.

To derive the $n^{-5/3}$ dependence of the resistivity, Thompson made a series of assumptions to deduce the carrier concentration. Since he did not measure the Hall coefficient of his samples, he assumed that the stoichiometry of his single crystals was the same as that for the powders the crystals were grown from and that each excess titanium atom donated four electrons to the conduction band. Our thermopower results agree with the last assumption (at least for $x > 0.01$), but the first assumption is suspect. We find no *a priori* reason to believe that the stoichiometry of the final crystal will be the same as the starting powder. Our lattice-constant measurements (see Sec. II) show that the c-axis lattice parameter of the most stoichiometric single crystals (including the Exxon sample) is considerably larger than Thompson *et al.*[2] report for their stoichiometric powders. Furthermore, the magnitude of the measured thermopower on the best samples is 10% below that for the stoichiometric powders.

These observations may mean that the stoichiometry of the crystals is different from the powders or that other sources of charge carriers (e.g., displacement defects) are introduced during single-crystal growth. In any case, the measurement of the Hall coefficient should provide a much more accurate value of the carrier concentration.

Our experimental results, therefore, contradict most of the previously quoted evidence for electron-electron scattering in TiS_2. The main attraction for electron-electron scattering was that it yielded a T^2 term in the electrical resistivity. However, our data show that T^2 is only approximately true only at high temperatures. Do our results rule out electron-electron scattering or could it still be the dominant mechanism and could the deviations from T^2 result from deviations from Matthiessen's rule or some other exotic effect?

Maldague and Kukkonen[23] have investigated the theory of electron-electron scattering in various types of systems. They found that in most cases the

T^2 term in the electrical resistivity appears only at low temperatures and disappears before it ever becomes the dominant temperature dependence. They found that only two mechanisms continue to yield a T^2 term in the resistivity at high T where the T^2 term is dominant. These are electron-electron umklapp scattering and electron-hole scattering in a compensated semimetal where the number of electrons equals the number of holes.

Using the semimetallic model of TiS_2 proposed by Thompson,[7] Kukkonen and Maldague[19] suggested that electron-hole scattering was a possible explanation of the T^2 resistivity. Since the present work shows that TiS_2 is not a semimetal, this explanation does not apply. Kukkonen and Maldague[19] also considered electron-electron umklapp scattering in TiS_2 and concluded that because the electron pockets (assumed to be on the facets of the hexagonal Brillouin zone) are so small and well separated, electron-electron umklapp scattering does not occur in TiS_2. This conclusion holds whether TiS_2 is a semiconductor or semimetal. Therefore the two specific carrier-carrier scattering mechanisms that could yield a T^2 resistivity at high T do not occur in TiS_2.

What scattering mechanism could produce a T^3 low-temperature resistivity and a roughly T^2 high-T resistivity with an $n^{-0.75}$ density dependence? Unfortunately we do not know. An $n^{-2/3}$ dependence of the resistivity can be obtained if the scattering matrix element is independent of n and the density of states is given by the free-electron relation $\rho(E_F) \propto n^{1/3}$. A constant matrix element occurs for electron-phonon scattering in nondegenerate semiconductors. In this case the deformation potential which enters the matrix element is independent of the number of electrons in the conduction band. On the other hand, for a free-electron metal the deformation potential is proportional to $E_F \propto n^{2/3}$ and this leads to an $n^{2/3}$ density dependence at high T. Although TiS_2 is a degenerate system, the density of electrons is only 1% that of typical metals. Therefore it is reasonable to expect that the deformation potential is the same as for a nondegenerate semiconductor. This would provide an explanation of the observed density dependence, but simple phonon scattering predicts the wrong temperature dependences.

Wilson[3,4] has suggested that the resistivity is due to Fivaz-mode homopolar optic-phonon scattering. Fivaz[24] and Fivaz and Mooser[25] considered optical-phonon scattering in layered nondegenerate semiconductors such as MoS_2. For homopolar modes they found that the dominant temperature dependence of the mobility was due to the number of thermally excited phonons,

$$\mu \propto \exp(\Theta_0/T) - 1 \ , \tag{7}$$

where Θ_0 is the temperature corresponding to the optical-phonon frequency. Fivaz and Mooser[25] approximated Eq. (7) by a power law near room temperature $T_0 = 300$ K,

$$\mu = \mu_0(T/T_0)^{-n} \ . \tag{8}$$

The exponent is the slope at T_0 in a plot of $\ln\mu$ vs $\ln T$:

$$n = \frac{\Theta_0/T_o \exp(\Theta_0/T_0)}{\exp(\Theta_0/T_o) - 1} \ . \tag{9}$$

Wilson noted that the homopolar optical mode in TiS_2 has $\Theta_0 = 480$ K. Taking $T_0 = 300$ K, Eq. (9) yields $n = 2.0$ and therefore T^2 resistivity. It is easily seen, however, that a T^2 law is a rather poor approximation to Eq. (7). The fit is only between 200 and 480 K. Below 100 K, the predicted resistivity equation (7) is exponentially small and cannot fit the low-temperature data. The theory of Fivaz and Mooser applies to nondegenerate semiconductors.

The temperature dependence of the resistivity due to optical-phonon scattering in a degenerate system is given by

$$\rho \propto [T \sinh^2(\Theta_0/2T)]^{-1} \ . \tag{10}$$

This result is easily derived from the variational expression for the resistivity and is independent of the exact nature of the electron-phonon coupling. Therefore it applies to both polar and nonpolar modes. It also applies to three-, two-, or one-dimensional systems. Like the result of Fivaz and Mooser, Eq. (10) is exponentially small below 100 K and cannot fit the TiS_2 data. Fitting a power law to Eq. (10), one finds an exponent of 1.4 near 300 K. These optical-phonon scattering formulas cannot fit the observed resistivity of TiS_2.

It is clear that none of the electron scattering mechanisms discussed above can explain the temperature dependence of the resistivity over the entire temperature range measured. Thus far, we concentrated on well-known scattering mechanisms and hoped to isolate one that could explain all the data. However, it is entirely possible that several mechanisms are acting together or that TiS_2 itself is sufficiently "strange" that phonon or electron-electron scattering produce different results in TiS_2 than they

do in simple metals. We do not consider the possibility of multiple mechanisms here, but we do briefly discuss the "strange" aspects of TiS_2.

In our discussion of scattering mechanisms, we have assumed that TiS_2 can be treated as a nearly ideal metal but, in fact, it is more nearly a dirty semiconductor. In the least stoichiometric samples, the density of carriers is approximately 4 times the number of excess titanium atoms. Even in our best samples, the residual resistivity remains very high. The electronic mean free path ($l = v_F\tau$) in sample no. 164 is 240 Å at 4.2 K, 12 Å at 300 K, and less than 2 Å at 700 K. For comparison, the mean free path in copper is more than 1000 times longer at 4.2 K and more than 300 times longer at 300 K. Furthermore, the scattering rate in TiS_2 is not small compared with the Fermi energy ($E_F = 0.06$ eV in sample no. 164); the ratio $\hbar/(\tau E_F)$ is about 0.1 at 4.2 K and greater than unity at 300 K.

Experimentally, TiS_2 appears to have some properties that are similar to those found in a highly doped semiconductor such as silicon or germanium doped with phosphorus, arsenic, or antimony.[26] These systems exhibit metal-insulator transitions. In the highly metallic region $n > 10^{18} - 10^{19}/\text{cm}^3$, these systems exhibit resistivities that vary as T^y where y is 2 for germanium doped with arsenic or silicon doped with phosphorus, y is $\frac{3}{2}$ for germanium doped with antimony.[26] These highly doped semiconductors also exhibit an anomaly in the magnetoresistance[27] similar to that we find in TiS_2.

The effect of electron-electron scattering on the resistivity of a disordered system has not been completely established. For weak disorder it is expected that Fermi-liquid theory will not change qualitatively and electron-electron scattering will continue to contribute a T^2 term. (In a highly disordered system, other temperature dependences are obtained.) We argued that electron-electron scattering does not contribute to the resistivity of TiS_2 because the normal scattering processes conserve wave vectors and umklapp scattering does not occur. In a disordered system wave vector is not defined, much less conserved. *If* wave-vector conservation could be abandoned, then normal electron-electron scattering would contribute a T^2 term to the resistivity at all temperatures, and normal electron-phonon scattering would contribute a T^3 term at low T instead of T^5. We emphasize the speculative nature of this idea and note again that there is no theory of this effect.

ACKNOWLEDGMENTS

This work was partially supported by National Science Foundation Grant No. DMR-78-07892 at Michigan State University and by NSF/MRL Program Grant No. DMR-77-23798 at Purdue University. We appreciate the assistance and expertise of J. L. Parsons in making the reflectivity measurements.

[1]S. Takeuchi and H. Katsuta, J. Jpn. Inst. Met. 34, 758 (1970); 34, 764 (1970).

[2]A. H. Thompson, F. R. Gamble, and C. R. Simon, Mater Res. Bull. 10, 915 (1975).

[3]J. A. Wilson, Solid State Commun. 22, 551 (1977).

[4]J. A. Wilson, Phys. Status Solidi 86, 11 (1978).

[5]R. H. Friend, D. Jerome, W. Y. Liany, J. C. Mikkelsen, and A. D. Yoffe, J. Phys. C 10, L705 (1977).

[6]C. H. Chen, W. Fabian, F. C. Brown, K. C. Woo, B. Davies, B. DeLong, and A. H. Thompson, Phys. Rev. B 21, 615 (1980).

[7]A. H. Thompson, Phys. Rev. Lett. 35, 1786 (1975).

[8]E. M. Logothetis, W. J. Kaiser, Carl A. Kukkonen, S. P. Faile, R. Colella, and J. Gambold, J. Phys. C 12, L521 (1979).

[9]E. M. Logothetis, W. J. Kaiser, Carl A. Kukkonen, S. P. Faile, R. Colella, and J. Gambold, in Proceedings of International Conference on Layered Compounds and Intercalates [Physica 99B, 193 (1980)].

[10]M. Bond, Acta Crystallogr. 13, 814 (1960).

[11]Our data from the ^{4}He cryostat exhibits a small hysteresis effect (0.4%) which was larger than the 0.1% accuracy of the experimental system. Upon temperature cycling, the temperature-independent part of the resistivity appears to change while the temperature-dependent part does not (down to ~ 2 K). The lowest-temperature data were taken during several temperature sweeps (typically $\gtrsim 5$ sweeps). The scatter in the data in Figs. 2(a) and 2(b) largely results from these shifts, and its magnitude (0.4%) is larger than the 0.1% accuracy of the experimental system. No systematics in these shifts were discernible with respect to time or with the size of the temperature excursion. At a fixed temperature, $\rho(0)$ is stable for times greater than an hour (longest time checked), whereas a temperature cycling might take as little as 15 min. The cause of these shifts remain unknown. The scatter in the data does not affect our conclusions, but prevents an accurate determination of the temperature dependence of the resistivity below about 4 K.

[12]G. Lucovsky, W. Y. Liang, R. M. White, and K. R.

Pirsharody, Solid State Commun. 19, 303 (1976).
[13]W. Y. Liang, G. Lucovsky, R. M. White, W. Stutius, and K. R. Pisharody, Philos. Mag. 33, 493 (1976).
[14]G. Lucovsky, R. M. White, W. Y. Liang, and J. C. Mikkelsen, Philos. Mag. 34, 907 (1976).
[15]L. A. Feldkamp, S. S. Shinozaki, C. A. Kukkonen, and S. P. Faile, Phys. Rev. B 19, 2291 (1979).
[16]J. A Benda, Phys. Rev. B 10, 1409 (1974).
[17]G. Lucovsky, private communication.
[18]See, for example, J. M. Ziman, *Electrons and Phonons* (Oxford University Press, London, 1972).
[19]C. A. Kukkonen and P. F. Maldague, Phys. Rev. Lett. 37, 782 (1976).
[20]C. A. Kukkonen and P. F. Maldague, Phys. Rev. B 19, 2394 (1979).
[21]N. J. Parada and G. W. Pratt, Jr., Phys. Rev. Lett. 22, 180 (1969).
[22]A direct plot of $\rho(300) - \rho(0)$ vs n_{Hall} is given in Ref. 9.
[23]P. F. Maldague and C. A. Kukkonen, Phys. Rev. B 19, 6172 (1979).
[24]R. Fivaz, J. Phys. Chem. Solids 28, 839 (1967).
[25]R. Fivaz and E. Mooser, Phys. Rev. 163, 743 (1967).
[26]M. J. Katz, S. H. Koenig, and A. A. Lopez, Phys. Rev. Lett. 15, 828 (1965).
[27]C. Yamanouchi, K. Mizuguchi, and W. Sasaki, J. Phys. Soc. Jpn. 22, 859 (1967).